JOURNAL OF APPLIED POLYMER SCIENCE VOL. 14, PP. 2239-2248 (1970)

# Energy Absorption in Polymeric Foams. I. Prediction of Impact Behavior from Instron Data for Foams with Rate-Independent Modulus

EBERHARD A. MEINECKE and DAVID M. SCHWABER,*
*Institute of Polymer Science, The University of Akron, Akron, Ohio 44304*

## Synopsis

The processes of energy dissipation in polymeric foams are discussed. Theoretical considerations and experimental results show that impact behavior of foams with a rate independent modulus can accurately be predicted by Instron data.

## INTRODUCTION

Foamed polymeric materials possess properties which make them applicable as impact absorbers. They can undergo large compressive deformations and absorb relatively large energies during a deformation cycle.[1] The stress–strain behavior of foams can be modified over a wide range to meet specific requirements by the choice of the matrix material as well as the form, size, and statistical distribution of the individual cells.[2] This advantageous combined effect of material properties and structure on the mechanical behavior of foams, however, complicates the description and prediction of their properties in terms of these parameters.

The most important attempts to predict polymeric foam properties from the constitutive equation of the matrix material and the foam structure include the cubic lattice model by Gent and Thomas,[3] which was later generalized to a random arrangement of foam strands,[4] and the model by Ko.[5] The application of models of foam structure can give a rough understanding of the contributions of the material properties as well as the structural design of the foam to the foam's mechanical behavior in the limits of the simplifying assumptions made. Although these models can predict Young's modulus for very small strains, they cannot explain satisfactorily the matrix buckling. This collapsing process is so complex that the nonlinear compressive response has to be expressed by an experimentally obtained strain function. This approach has been applied by Rusch.[6] The deformation stress, $\sigma$, is considered to be the product, as described by eq. (1), of a function of strain alone and another which is dependent on properties of the foam structure and the matrix material:

$$\sigma = E_t \epsilon \psi(\epsilon) \tag{1}$$

* On leave of absence from Monarch Rubber Company, Inc., Baltimore, Maryland.

Where $E_f$ is the apparent Young's modulus of the foam, $\epsilon$ is the compressive strain, and $\psi(\epsilon)$ is a factor reflecting the collapse of the matrix. These empirical equations can be useful in determining the foam parameters necessary for a desired deformation behavior. It has been pointed out, however, that both of these approaches to explain the very complex deformation behavior of foams are limited in their accuracy.

In this series of papers, emphasis would be placed on the interrelation of foam behavior in different types of tests rather than on the correlation of mechanical behavior of foams with their structure and material properties. The responses of a foam to impact, sinusoidal loading, and constant rate deformation are related, and one response can be predicted from data obtained in another test. These relations between tests are quite simple for foams with little energy dissipation due to pneumatic damping, and for foams made of a material the glass transition temperature of which is well above or below testing temperature. For such materials, the energy loss in dynamic tests, expressed as tan $\delta$ or as hysteresis, is nearly independent of frequency or rate over a wide frequency range.[7] It is possible, therefore, to compare directly deformation energies, hysteresis, etc., observed during tests with constant rates (Instron test) with those during tests with varying velocity (impact, sinusoidal vibrations). This comparison is more complicated for materials close to the transition zone, where energy dissipation is strongly rate dependent. This rate dependence limits the direct comparison of data obtained at one velocity with the impact data, since in this test the rate of deformation decreases with penetration distance. The Boltzmann superposition principle has to be applied. The same considerations have to be made for foams of small cell size and for high deformation rates, since the deformation energies and forces are affected by rate-dependent components arising from the compression and the viscous flow of air through the pores.[8]

## EXPERIMENTAL

Impact and constant rate stress–strain curves were obtained on commercial reticulated polyurethane foams by Scott. Three cell sizes were used: 10, 30, and 60 pores per inch (ppi). The density of all three foams was between 0.0258 and 0.0296 g/cm$^3$. The glass transition temperature of the polyurethan is about $-45$°C,[9] i.e., well below the testing temperature.

The impact properties were obtained with the help of a modified Scott pendulum (Fig. 1). The potential energy could be changed by added weights on the pendulum as well as by different angles of drop, thus providing a combination of different impact velocities and kinetic energies before impact.

The pendulum velocity during impact was recorded with the help of a LVDT (Schaevitz 500SS-LT) the core of which was attached to the pendulum. It enters the LVDT shortly before impact. The LVDT was connected to a 2.5-kHz power supply demodulator (Schaevitz CA2500)

with a frequency response of 250 Hz at ± 1 dB. The output of the demodulator was fed into an oscilloscope (Textronix 564B). Static calibrations of the oscilloscope readings were performed with shims of known thicknesses placed between the hammer and the anvil. The velocities before impact were compared with those calculated from the drop height $h$ of the pendulum:

$$v_{\text{ideal}} = \sqrt{2gh} \tag{2}$$

The differences can be attributed to friction in the pendulum, especially since they were proportioned to the drop height.

The pendulum consisted of a thin-walled aluminum tube and was subject to large vibrations due to the shock of impact. These vibrations distorted

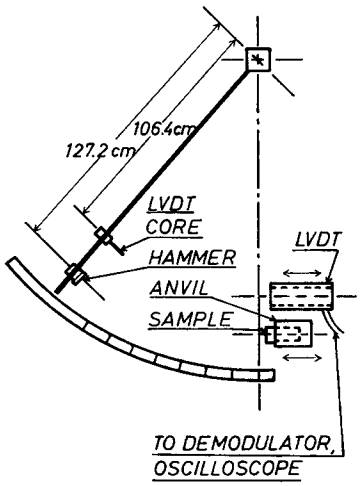


Fig. 1. Schematic representation of impact pendulum.

oscilloscope readings and dissipated energy. The pendulum was reinforced with guy wires to increase the moment of inertia of the structure and thereby increase the stiffness without greatly increasing the mass. The energy loss due to the slight remaining vibrations of the pendulum rod after impact and a possible movement of the anvil was determined with identical coil springs being put between anvil and hammer. Since the loss was proportional to the number of springs used, the energy loss due to the pendulum inaccuracies was determined by extrapolation to zero number of springs from a plot of the energy loss versus the number of springs. Another energy loss arose from a catcher holding the pendulum at maximum rebound angle. The data reported later have been corrected for these energy losses.

A table model Instron tester was used to obtain stress–strain curves at different constant deformation rates. All tests were performed at room temperature.

## RESULTS

Typical data obtained at constant rate of compression at the Instron tester are shown in Figures 2 and 3. The data presented in these figures were obtained for one maximum strain at different rates of compression ratios between 0.5 and 20 cm/min. Presented in Figure 2 are data for the 10-ppi foam; in Figure 3, for the 60-ppi foam. It is apparent that the stress–strain curve is not affected by rate at these rates and testing temperatures, indicating that the response of the matrix material is rate independent and that air flow does not contribute significantly to the load.

The Instron traces shown in Figure 4 were obtained at one speed (2 cm/min) on the same sample. The sample was first compressed to a strain of $-10\%$. Then the crosshead was instantaneously reversed until

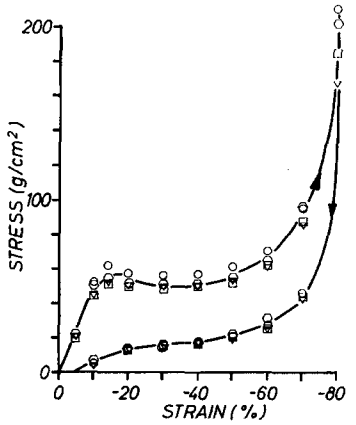


Fig. 2. Stress–strain behavior of foams with 10 ppi at constant loading and unloading rates: (▽) 0.5 cm/min; (□) 2.0 cm/min; (○) 5.0 cm/min; (○) 20.0 cm/min.

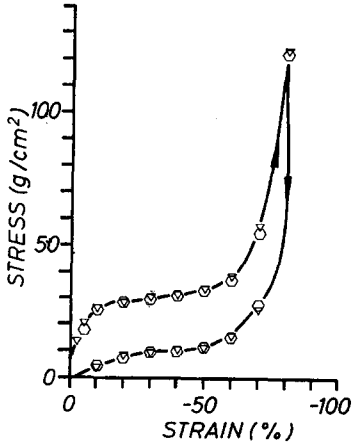


Fig. 3. Stress–strain behavior of foams with 60 ppi at constant loading and unloading rates: (▽) 0.5 cm/min; (○) 20 cm/min.

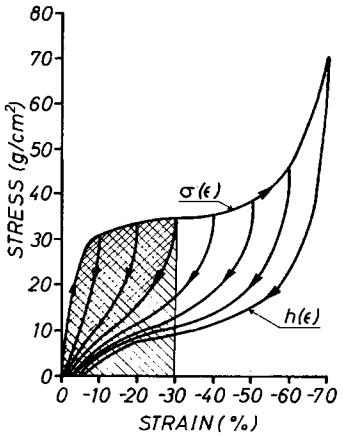


Fig. 4. Example of energy to deform and hysteresis for sample loaded and unloaded at constant rate.

it reached its original position. After 5 min the sample was compressed to a strain of $-20\%$ and got then another chance to relax for 5 min. This procedure on this example was repeated until a strain of $-70\%$ was reached, although normally data were recorded to a strain of $-90\%$. It was found that this test procedure yields the same loading and unloading curve for any strain as a test on a sample not previously compressed to smaller strains. This behavior is not necessarily typical for low density polyurethane foams. Since this foam was reticulated by the explosion technique, its structure was ruptured severely. It can normally be observed that the stress–strain curve for unreticulated foams during the first compression cycle is different from the one during subsequent cycles.

Figure 2 shows a compressive stress–strain curve that is linear up to about 10% compression. This type of foam typically exhibits linearily up to only 3% or 4%. This behavior could result from the large cell size combined with small specimen size, which makes the dimensions of the foam and hence the strain indeterminate. Figure 10 shows stress–strain curves for samples of various thicknesses from 2 cm to 10 cm. Although the general shape and magnitude of the stress–strain curves are similar, there is an obvious effect of sample size at small strains. These data appear to show that the apparent linear limit is shifted to smaller strains as specimen thickness is increased. For the 10-cm specimen, the linear limit is about 5%, half of that observed for the 2-cm specimen. (This test cannot be performed this way with a strongly viscoelastic material or one exhibiting yielding.)

In Figure 4, the stored energy and the hysteresis can be easily obtained from the area under the loading curve and the area between the loading and unloading curve, respectively, as indicated by the cross hatchings.

Typical data obtained with the pendulum are shown in Figure 5 for two different foams of 30 ppi and 60 ppi and two initial positions of the pendu-

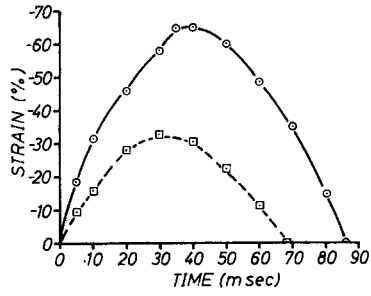


Fig. 5. Strain vs. time for impact-loaded samples: (⊙) 30 ppi, 8.5°; (⊡) 60 ppi, 5.5°.

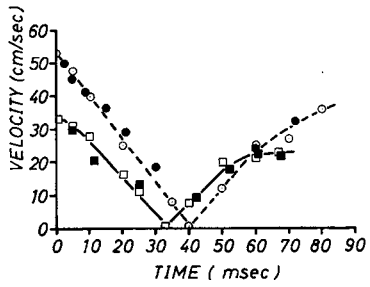


Fig. 6. Dependence of velocity on time after impact from data of Figures 4 and 5: (⊙), (●), 30 ppi, 8.5°; (□), (■) 60 ppi, 5.5°.

lum, 8.5° and 5.5°. These data were taken from the storage oscilloscope, corrected for nonlinearities of the LVDT and reduced to strain from the original distance-versus-time plot. The kinetic energy of the pendulum before impact,

$$E_d = {}^1/_2\, m v_m^2, \tag{3}$$

(where $m$ and $v_m$ are the total mass and reduced velocities of the single masses of the pendulum, respectively) can be obtained from the slope of the strain profiles at zero time. Similarly, one obtains the energy after impact $E_d$, and the energy lost during impact, $E_h$:

$$E_h = {}^1/_2\, m(v_{\text{in}}^2 - v_{\text{out}}^2) \tag{4}$$

The energies obtained from the slopes of these strain profiles were compared with the potential energies of the pendulum in the rest state:

$$E_d = mgl_{cg}\,(1\text{-}\cos\theta_i) \tag{5}$$

$$E_h = mgl_{cg}\,(\cos\theta_i\text{-}\cos\theta_r) \tag{6}$$

where $g$ is the acceleration due to gravity, $l_{cg}$ is the distance from the pendulum fulcrum to the center of gravity, and $\theta_i$ and $\theta_r$ are the angles of the pendulum initially and on recovery, respectively.

The maximum penetration of the hammer can easily be read from the curves. Once the velocity profile is obtained from the strain-versus-time

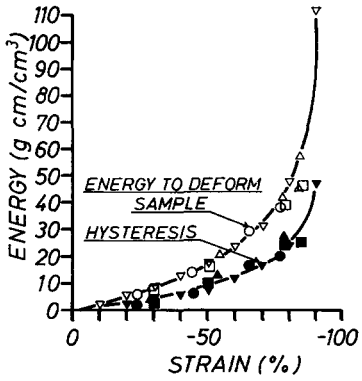


Fig. 7. Energy to deform and hysteresis for strained samples of 10 ppi-foam; (▽) Instron; (○) $m_p$ = 2.06 kg; (□) $m_p$ = 2.38 kg; (△) $m_p$ = 2.61 kg.

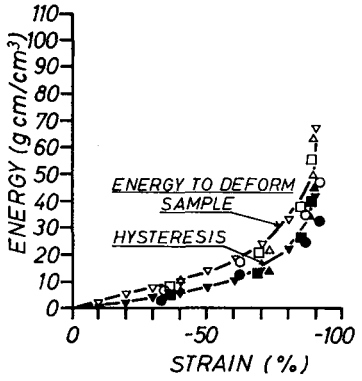


Fig. 8. Energy to deform and hysteresis for strained samples of 30 ppi-foam: (▽) Instron; (○) $m_p$ = 2.06 kg; (□) $m_p$ = 2.38 kg; (△) $m_p$ = 2.61 kg.

curves, the deceleration of the pendulum can be obtained from the slopes of this curve (Fig. 6). This two-step procedure yields results with considerable scatter, however. The acceleration should be obtained, therefore, with the help of an accelerometer attached to the pendulum.

Data as presented in Figure 4 were taken for all three sample types with different impact velocities and different kinetic energies before impact. The energy to deform the samples to their maximum strain (the deformation energy $E_d$) and the energy lost during impact (the hysteresis $E_h$) were determined from these graphs and plotted versus $\delta$ maximum strain (Figs. 7, 8, and 9).

A problem faced in the experimentation is lack of uniformity from one sample to another. Samples compared in one set of data were normally identical, or else experiments were repeated on one sample. Major changes were found when testing samples produced in different lots by the manufacturer. The energy–strain curves in Figures 7 and 9 are virtually identical, while the "plateau stress" for the 10-ppi foam (Fig. 2) is almost twice that

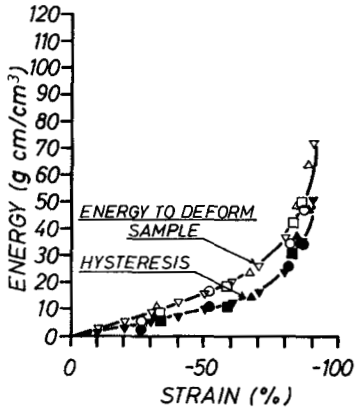


Fig. 9. Energy to deform and hysteresis for strained samples of 60 ppi-foam: (▽) Instron; (○) $m_p$ = 2.06 kg; (□) $m_p$ = 2.38 kg; (△) $m_p$ = 2.61 kg.

of the 60-ppi foam (Fig. 3). This large discrepancy is due to the fact that the foams used to calculate Figures 2 and 7 are different. They are both 10-ppi foams but were obtained at different times.

## DISCUSSION

The Instron data in Figures 2 and 3 indicate that the modulus of the polyurethane foams studied is independent of rate at room temperature for the velocity ranged covered. It can therefore be expected, as previously indicated, that the stress–strain behavior of these foams will be the same for other loading histories, for example the impact test, where the deformation rate is changing from $v_{in}$ to 0 to $v_{out}$; i.e., the stored energy is a function of strain only for a given sample.

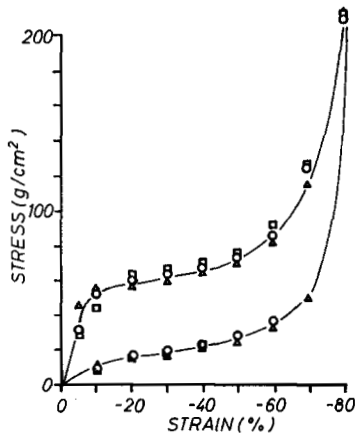


Fig. 10. Stress–strain behavior of samples of 10-ppi foam with varying sample thickness: (△) 10 cm; (○) 5 cm; (□) 2 cm. 20.0 cm/min.

The stored energy data obtained from the impact tests were compared to data calculated from the Instron tracings and are plotted for comparison in Figures 7, 8, and 9. Excellent agreement, though some scatter, is found. The scatter of the energy data derived from the Instron tests arises mostly from inaccuracies in determining the areas under the stress–strain curves with the help of a planimeter, while the accuracy of the energies obtained from impact data is limited by the determination of the slopes. These data are, however, more accurate than the ones obtained in the conventional way from the heights of the pendulum when friction losses are not considered. If, for example, the pendulum is dropped from a height of 5 cm, then the velocity before impact is due to friction 10% lower than calculated, i.e., the energy is lower by 23%.

It is possible to obtain from the Instron data more information about the behavior during impact. The maximum strain can be read directly from Figures 7, 8, and 9 for known kinetic energies before impact. The velocity of the pendulum after impact and the deceleration and following acceleration versus time (or penetration distance) can also be obtained.

In Figure 6, the pendulum velocities after impact for two different foams and kinetic energies before impact have been plotted against time. Values obtained from distances-versus-time data of an impact test as shown in Figure 5 are compared with data obtained from an Instron test. The equivalence of kinetic and potential energy for this foam system permit the calculation of velocity versus time from eqs. (7) and (8), where the energy-versus-distance function is obtained from data as shown in Figure 4.

Compression:

$$v_x = \frac{2}{m}\left\{\frac{1}{2}mv_{\text{in}}^2 - \int_0^x \sigma(\epsilon)\, d\epsilon\right\}^{1/2} \tag{7}$$

Recovery:

$$v_x = \frac{2}{m}\left\{\int_x^{x_{\max}} h(\epsilon) d\epsilon\right\}^{1/2} \tag{8}$$

where $\sigma(\epsilon)$ is the stress during loading, $h(\epsilon)$ is the stress during unloading (Fig. 4), and $x_{\max}$ is the maximum penetration of impact. It is interesting to note that the deceleration is remarkably constant with time for the foams investigated. This phenomenon is due to the plateau region as in Figure 4 of the stress–strain curve, where

$$\text{stress} = \frac{\text{force}}{\text{area}} = mx \tag{9}$$

and a constant force would yield a constant deceleration.

The deceleration is a most useful value to obtain for materials from an engineering point of view. This paper describes all impact data in terms of energy, velocity, and displacement. In comparing stress–strain to impact

behavior, we find it not precise to graphically differentiate the strain–time curves twice to obtain the acceleration values.

## CONCLUSIONS

In special cases, the response of a foam to impact loading can be accurately predicted from loading-unloading stress–strain data obtained at constant strain rate (Instron test) and a variety of maximum strains. This prediction is accurate only for foams the matrix material of which has approximately rate independent mechanical behavior. In addition, contributions to the deformation and loss energies of the foam due to viscous flow through the pores has to be negligible; i.e., the pores have to be relatively large, and the strain rates and sample dimensions reasonably small. The prediction of impact behavior for foams not subject to these restrictions will be discussed in a forthcoming publication.

## References

1. E. Baer, Ed., *Engineering Design for Plastics,* Reinhold, New York, 1964, p. 1006.
2. R. Chan and M. Nakamura, *J. Cell. Plastics,* **5,** 112 (1969).
3. A. N. Gent and A. G. Thomas, *Rubber Chem. Tech.,* **36,** 597 (1965).
4. A. N. Gent and A. G. Thomas, *J. Appl. Polym. Sci.,* **1,** 107 (1959).
5. W. L. Ko, *J. Cell. Plastics,* **1,** 45 (1965).
6. K. C. Rusch, *J. Appl. Polym. Sci.,* **13,** 2297 (1969).
7. A. B. Davey and A. R. Payne, *Rubber in Engineering Practice,* London MacLaron, 1964, pp. 24–38.
8. A. N. Gent and K. C. Rusch, *Rubber Chem. Tech.,* **39,** 389 (1966).
9. C. W. Kosten and C. Zwikker, *Mededelingen van de Rubber-Stichting,* **6,** (1938); *Rubber Chem. Tech.,* **12,** 105 (1939).
10. J. F. Pizzirusso, Scott Paper Company, Foam Division, personal communication.

Received June 1, 1970